Parametric and structural optimization of the modal filter on a double-sided printed circuit board

Parametric and structural optimization of the modal filter on a double-sided printed circuit board

M A Samoylichenko and T R Gazizov
Tomsk State University of Control Systems and Radioelectronics, 40, Lenina ave., Tomsk, 634050, Russia.

E-mail: 1993mary2011@mail.ru, talgat@tu.tusur.ru

Abstract. The effect of reducing the foil thickness and removing of one or two reference conductors in a modal filter on a double-sided printed circuit board is considered. The simulation of the ultra-short pulse propagation in such structures demonstrated that the signal is attenuated by 2 times in relation to half the e.m.f. when the foil thickness is 70 μm and by 3 times when the top left reference conductors is removed.

1. Introduction

Today's radio electronic equipment (REE) is increasingly equipped with electronic control systems and microprocessor-based devices that are sensitive to electromagnetic interference. An increase in the degree of integration of the electronics element base leads to a decrease in the electrical strength of individual components of the equipment, as well as an increase in the vulnerability of REE elements to electromagnetic interference of different origins. In particular, ultrashort pulses (USPs) can lead to REE failure or malfunction [1].

The spacecraft onboard equipment is sensitive to USPs. In addition to general requirements (noise immunity, reliability, electromagnetic compatibility, etc.), a number of specific requirements are imposed on spacecraft onboard equipment: low mass, compactness, low power consumption, reliability under conditions of high temperatures, vibrations and overloads, immunity to penetrating radiation and low external pressure. Therefore, devices protecting against dangerous USPs, which are now being developed, must meet all these requirements. New protective devices called modal filters (MF) are the example of such devices [2]. They decompose an USP in a segment of a coupled line into modes each of which propagates with its own delay, so the MF output pulses have smaller amplitude. For example, such MF configurations as a multiconductor line, an interdigitated structure, a mirror-symmetric MF have been investigated [3-9]. However, they are difficult to integrate into double-side printed circuit boards (PCBs). This leads to the fact that they must be made as separate protective devices. Therefore, the search for new MF structures, which are free from this disadvantage, is relevant. One of the simple options for implementation is an MF cut in a double-sided PCB. It is noteworthy that for such an MF it is possible to lower the mass and to achieve the attenuation of the USP by reducing, for example, only the thickness of the conductors, but also by removing one or two reference conductors. The purpose of this work is to explore these possibilities.

2. Structure under investigation

Figure 1*a* shows the cross-section of the original MF with the following parameters: ε_r is the relative permittivity, *w* is the width of the conductors, *t* is the thickness of the conductors, *h* is the substrate thickness, *s* is the separation between the conductors. The foil-clad fiberglass (ε_r=4.5) was chosen as the substrate material because of its low cost.

Optimization of MF parameters is performed according to the following criteria - the increase of the difference of the per-unit-lenght delays and the alignment of the USP amplitudes. This allows a uniform decomposition of the input influence with longer duration.

The MF connection diagram is shown in Figure 1*a*. The active conductor is connected to a pulse signal source, represented in the circuit as an ideal e.m.f. source *E* and internal resistance *R*1. The other end of the active conductor is connected to load *R*3. The resistance values *R*1, *R*2, *R*4, *R*5 were assumed to be the same and equal to 50 Ω. The input excitation was a trapezoidal pulse with parameters: the e.m.f. amplitude of 2 V; the rise, flat peak and fall times of 50 ps each. The parameters and waveforms were calculated using the quasistatic approach in the TALGAT software [10]. The losses in the conductors and dielectrics were not taken into account.

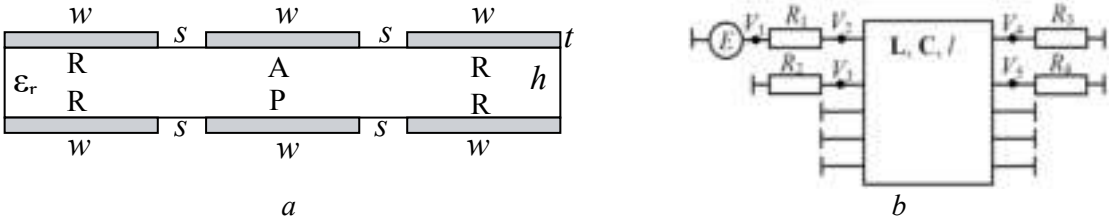

Figure 1. MF cross section (*a*), where the conductors: R – reference, A – active, P – passive, and MF connection diagram (*b*)

3. Simulation results

Since in this work the influence of *t*, and the presence of reference conductors at this stage of the simulation *h*, *w* and *s* are chosen arbitrarily. The simulation was performed with *h*=500 μm, *w* (for each conductor)=1000 μm, *s*=300 μm, MF length (*l*) of 1 m, *t*=105, 70, 35, 18 μm. The calculated matrices of per-unit-length delay parameters for *t*=105 μm are the following:

$$\mathbf{C}=\begin{bmatrix} 139.7 & -21.36 & -21.36 & -79.62 & -8.754 \\ -21.36 & 118.2 & -2.198 & -8.734 & -1.246 \\ -21.36 & -2.198 & 118.2 & -8.734 & -84.80 \\ -79.62 & -8.734 & -8.734 & 139.8 & -21.31 \\ -8.754 & -1.246 & -84.80 & -21.31 & 118.3 \end{bmatrix} \text{ pF/m;} \quad \mathbf{L}=\begin{bmatrix} 508.853 & 203.655 & 370.556 & 308.559 & 336.548 \\ 20.655 & 352.76 & 183.281 & 149.265 & 169.73 \\ 370.556 & 183.281 & 686.56 & 316.081 & 503.361 \\ 308.559 & 149.265 & 316.081 & 454.295 & 336.375 \\ 336.548 & 169.73 & 503.361 & 336.375 & 672.752 \end{bmatrix} \text{ nH/m.}$$

The results of simulating the voltage waveforms at the MF input and output are shown in Figure 2. We can see that with *t*=105 μm (Figure 2*a*) and 70 μm (Figure 2*b*), 3 pulses are observed at the MF output. This is explained by the fact that the amplitudes of the first and fourth pulses are small. For *t*=35 μm (Figure 2*c*) and *t*=18 μm (Figure 2*g*) the amplitude of the first pulse becomes larger and it is clearly visible. The amplitude of the fourth pulse also becomes larger, but due to partial overlapping of the third pulse (for *t*=35 μm the difference of the per-unit-length is $\tau_4-\tau_3$=0.184 ns/m), it is almost unobservable. The amplitude of the fifth pulse (which is the maximum one) becomes lowest for *t*=70 μm. The obtained values of per-unit-length delays and pulse amplitudes are given in Table 1.

Table 1. Per-unit-length delays (τ_i, ns/m) and amplitudes (U_i, V) for different values of *t*

***t*, μm**	τ_1	τ_2	τ_3	τ_4	τ_5	U_1	U_2	U_3	U_4	U_5
105	4.199	4.597	5.786	5.941	6.411	–	0.208	0.306	–	0.494
70	4.353	4.744	5.721	5.931	6.474	–	0.233	0.326	–	0.428
35	4.382	4.924	5.811	5.995	6.477	0.016	0.220	0.285	–	0.480
18	4.418	4.939	5.858	6.024	6.497	0.009	0.223	0.286	–	0.478

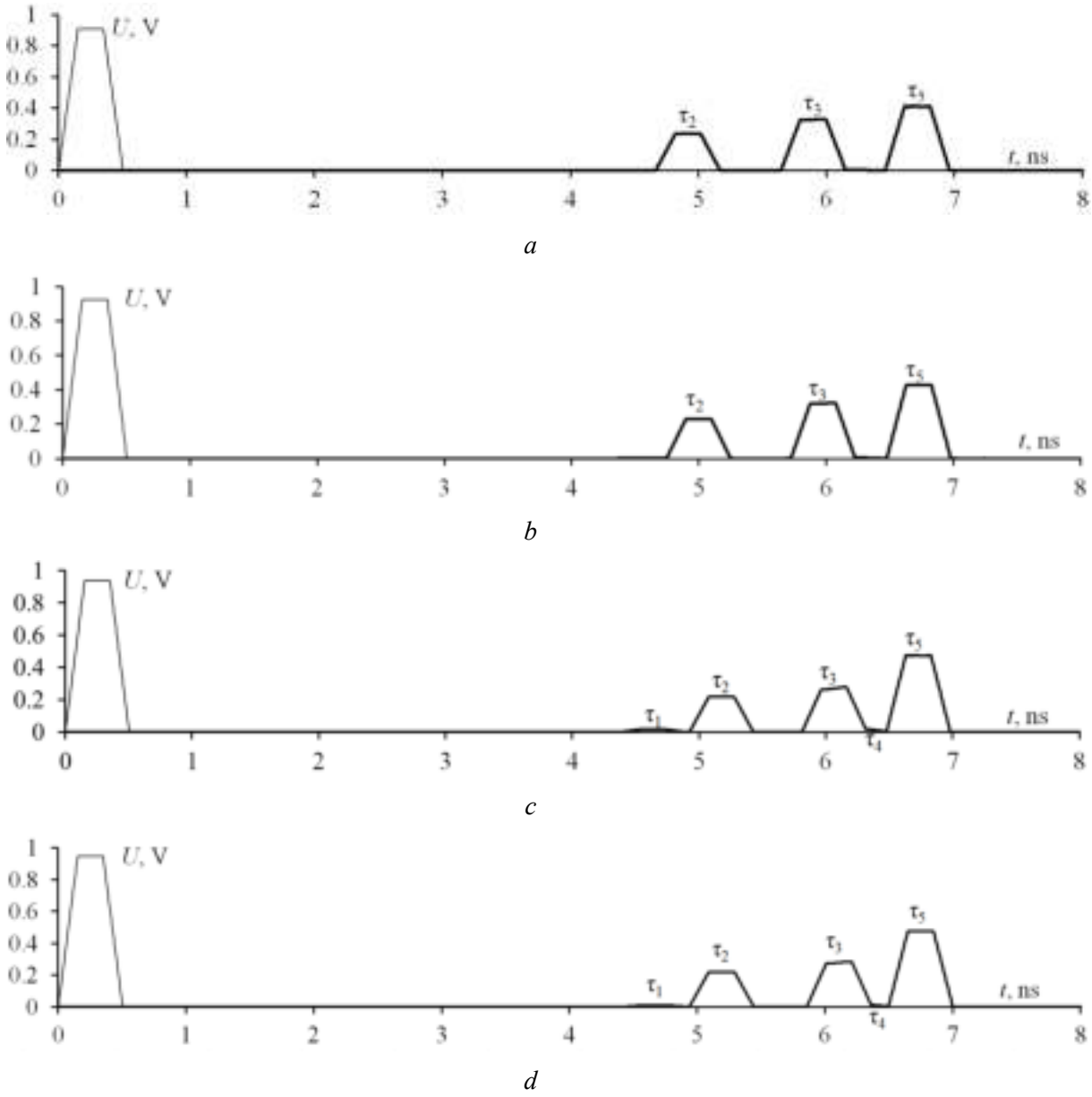

Figure 2. Voltage waveforms at the MF input (–) and output (**-**) for t=105 (*a*), 70 (*b*), 35 (*c*) and 18 μm (*d*)

When the reference conductors were removed, the simulation was performed with the following parameters: w=1000 μm, s=300 μm, h=500 μm, t=105 μm. We considered four cases.

The cross section of the MF without the lower left reference conductor is shown in Figure 3*a*, and the connection diagram is shown in Figure 3*b*. The results of simulating the input and output voltage waveforms for such MF configuration are shown in Figure 4.

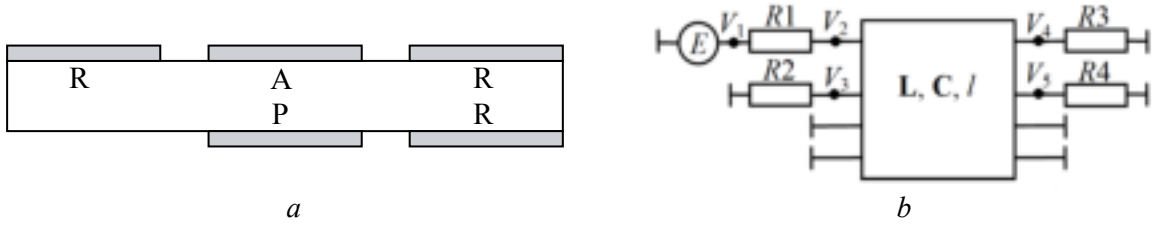

a *b*

Figure 3. Cross section (*a*) and connection diagram (*b*) of the MF without the lower left reference conductor

The obtained values of per-unit-length delays and pulse amplitudes are given in Table 2.

Table 2. Per-unit-length delays (τ_i, ns/m) and amplitudes (U_i, V) for are MF without the lower left reference conductor

τ_1	τ_2	τ_3	τ_4	U_1	U_2	U_3	U_4
4.399	4.751	5.736	6.358	–	0.307	0.191	0.501

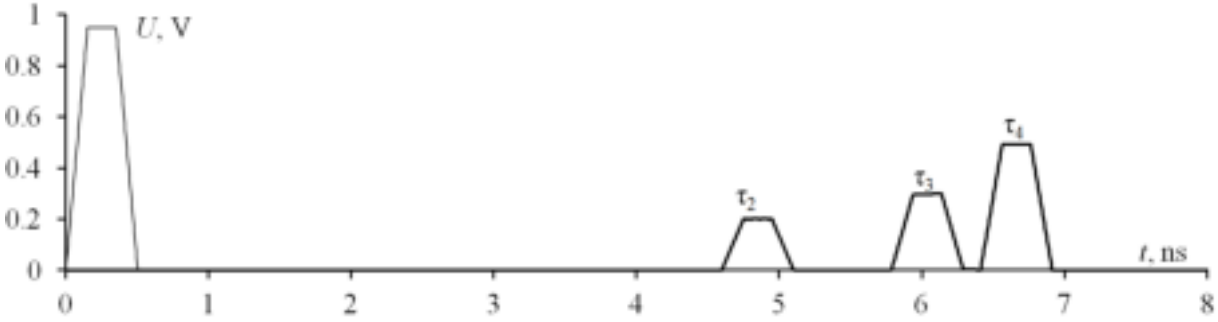

Figure 4. Voltage waveforms at the input (–) and output (-) of the MF without the lower left reference conductor

The cross section of the MF without the upper left reference conductor is shown in Figure 5, and the connection diagram is shown in Figure 3*b.* The results of simulating the input and output voltage waveforms for such MF are shown in Figure 6.

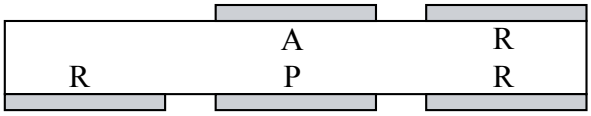

Figure 5. Cross section of the MF without upper left reference conductor

The obtained values of pulse amplitudes and per-unit-length delays are given in Table 3.

Table 3. Per-unit-length delays (τ_i, ns/m) and amplitudes (U_i, V) for the MF without upper left reference conductor

τ_1	τ_2	τ_3	τ_4	U_1	U_2	U_3	U_4
4.401	4.751	5.736	6.358	0.037	0.127	0.237	0.609

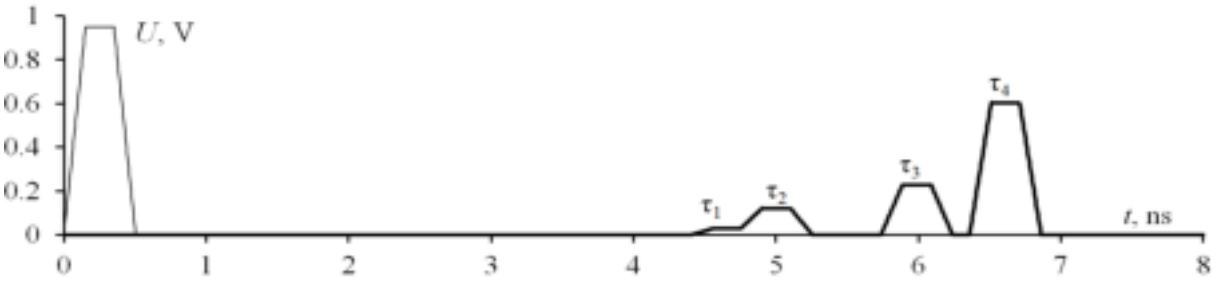

Figure 6. Voltage waveforms at the input (–) and output (-) of the MF without upper left reference conductor

The cross section of the MF without the upper right reference conductor is shown in Figure 7, and the connection diagram is shown in Figure 3*b*. The results of simulating the input and output voltage waveforms of such MF are shown in Figure 8.

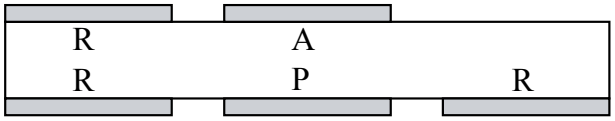

Figure 7. Cross section of the MF without the upper right reference conductor

The obtained values of pulse amplitudes and per-unit-length delays are given in Table 4.

Table 4. Per-unit-length delays (τ_i, ns/m) and amplitudes (U_i, V) for the MF without the upper right reference conductor

τ_1 ns/m	τ_2 ns/m	τ_3 ns/m	τ_4 ns/m	U_1 V	U_2 V	U_3 V	U_4 V
4.398	4.750	5.736	6.359	0.070	0.334	0.216	0.325

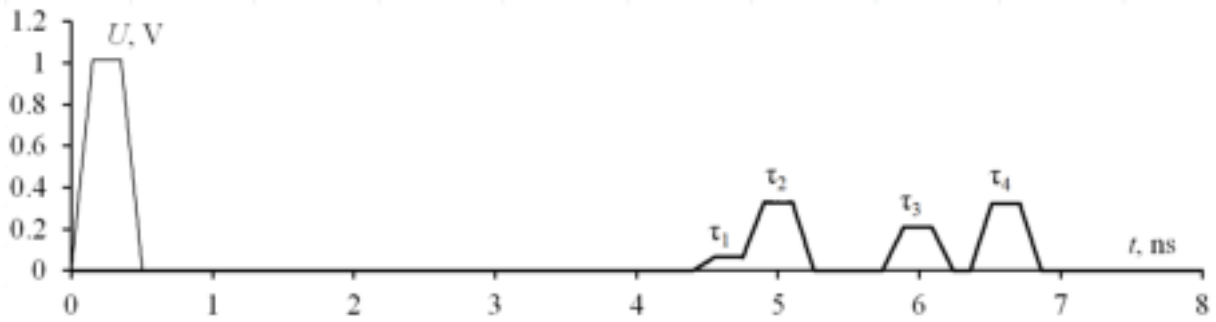

Figure 8. Voltage waveforms at the input (–) and output (-) of the MF without the upper right reference conductor

The presented results show that when one of the reference conductors is removed from the top, at the MF output we can observe 4 pulses, whereas when the lower reference conductor is removed, there are 3 pulses, which is explained by the small amplitude of the first pulse. The removal of the upper right reference conductor reduced the maximum amplitude. With t=105 μm and all reference conductors, the maximum amplitude is equal to 0.494 V, while when the right upper reference conductor is removed, the maximum amplitude is equal to 0.334 V. We can see that the best result is achieved when the right conductor is removed from the top, because U_1=0.070 V, U_2=0.334 V, U_3=0.216 V and U_4=0.325 V, and the differences in the per-unit-length delays are: τ_4–τ_3=0.623 ns/m, τ_3–τ_2=1.236 ns/m and τ_2–τ_1=0.352 ns/m. The removal of the left reference conductor, both upper and

lower, only affects the amplitude. Thus, when removing the upper conductor, we get U_1=0.037 V, U_2=0.127 V, U_3=0.237 V and U_4=0.609 V, and when removing the lower one, we get U_2=0.307 V, U_3=0.191 V and U_4=0.501 V. The differences in the per-unit-length delays for two cases are the same and equal: $\tau_4-\tau_3$=0.622 ns/m, $\tau_3-\tau_2$=0.985 ns/m and $\tau_2-\tau 1$=0.352 ns/m.

At last, the cross section of the MF without two reference conductors is shown in Figure 9*a* and the connection diagram is shown in Figure 9*b*. The results of simulating the voltage waveforms at the MF input and output are shown in Figure 10. We can see that the input signal is decomposed into a sequence of two pulses.

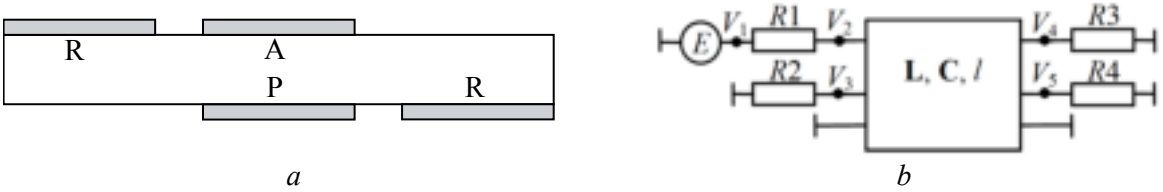

a *b*

Figure 9. Cross section (*a*) and connection diagram (*b*) of the MF without two reference conductors diagonally

The obtained values of per-unit-length delays and pulse amplitudes are given in Table 5.

Table 5. Per-unit-length delays (τ_i, ns/m) and amplitudes (U_i, V) for the MF without two reference conductors diagonally

τ_1	τ_2	τ_3	U_1	U_2	U_3
4.524	4.80013	6.20316	–	0.160	0.817

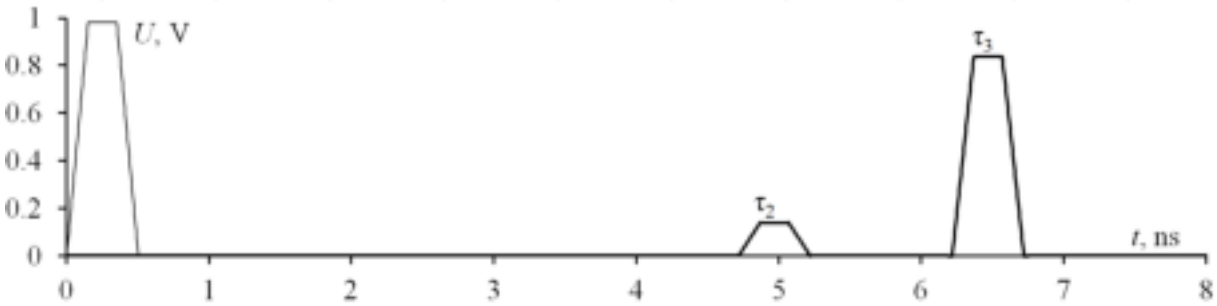

Figure 10. Voltage waveforms at the input (–) and output (-) of the MF without two reference conductors diagonally

4. Conclusion

Thus, it is shown that by reducing the mass of the MF cut in the double-sided PCB it is possible to achieve greater attenuation of the USP. So, by reducing the conductor thickness to t=70 μm, we achieved the attenuation by 2 times in relation to half the e.m.f., and by removing the top right reference conductor - by 3 times. It is not insignificant that the considered variants of MF implementation allow to reduce mass (at the expense of removal of one reference conductor the mass of conductors is reduced in 1.6 times) that is actual and important in the onboard equipment of a spacecraft. The findings make further research on mass reduction in such MFs relevant. Also, to achieve the best result, it is reasonable to perform additional parametric optimization for each of the considered configurations.

Acknowledgments

The reported study was funded by RFBR, project number 19-37-51017.

References

[1] Gizatullin Z M and Gizatullin R M 2016 *Journal of Communications Technology and Electronic*s **61 (5)** 546–550
[2] Gazizov T R and Zabolotsky A M 2007 *Proc. of the 18-th Int. Zurich Symp. on EMC* pp 273–276
[3] Khazhibekov R and Zabolotsky A M 2019 *Int. Siberian Conf. on Control and Communications* pp 1–4
[4] Chernikova E, Belousov A and Zabolotsky A M 2019 *Int. Siberian Conf. on Control and Communications* pp 1–4
[5] Belousov A, Zabolotsky A M and Gazizov T T 2017 *18th Int. Conf. of Young Specialists on Micro/Nanotechnologies and Electron Devices* pp 46–49
[6] Khazhibekov R, Zabolotsky A M and Khramtsov M V 2017 *Proc. of IEEE 2017 Int. multi-conf. on engineering, computer and information science* pp 506–509
[7] Belousov A O 2020 *21st International conference of young specialists on micro/nanotechnologies and electron devices* pp 118–122
[8] Khazhibekov R and Zabolotsky A 2019 *20th International conference of young specialists on micro/nanotechnologies and electron devices* pp 88–91.
[9] Khazhibekov R R, Zabolotsky A M, Zhechev Y S, Kosteletskii V P and Gazizov T R 2019 *IOP Conference Series: Materials Science and Engineering* **560 (1)** 012145
[10] Kuksenko S P 2019 *IOP Conference Series: Materials Science and Engineering* **560 (1)** 012110